International Research Journal of Engineering and Technology (IRJET) e-ISSN: 2395 -0056
Volume: 02 Issue: 06 | Sept-2015 www.irjet.net p-ISSN: 2395-0072

ENHANCED PERFORMANCE OF OPTICAL OZONE SENSORS USING Au@Ag CORE-SHELL THIN FILM NANOISLANDS

Satish Addanki[1] and D. Nedumaran[2*]

[1, 2] Central Instrumentation and Service Laboratory
University of Madras, Guindy Campus, Chennai – 600025, TN, India

---

Abstract - Nanosensors play a vital role in the detection of atmospheric ozone. In this paper, we present an optical sensor for the detection of ozone on the Au@Ag core-shell thin film nanoislands using Surface Plasmon Resonance technique. First, we implemented the simulation in a COMSOL Multiphysics 4.2 and MATLAB environment. Then, we extended the work to fabricate Au@Ag core-shell thin film nanoislands using APTMS and PVA as binding agents. We analyzed the simulation and fabrication results for the detection of ozone on Au@Ag core-shell thin film nanoislands. The fabricated sensors were characterized using SEM, AFM for morphological analysis. The optical and resistive responses of the Au@Ag core-shell thin film nanoislands were analyzed. In this study, the APTMS based Au@Ag core-shell thin film nanoislands exhibited better response towards ozone sensing than the PVA mixed Au@Ag core-shell thin film nanoislands.

Key Words: *Au@Ag core-shell nanoparticles, APTMS ((3-Aminopropyl)trimethoxysilane), PVA, Absorbance, Optical Sensor, Surface Plasmon Resonance (SPR).*

1. Introduction

Optical sensors were developed for gas sensing applications using the Surface Plasmon Resonance (SPR) technique [1]. Gold and silver have many important characteristics lying within the visible region, like good reflectivity properties and interactions with an electromagnetic wave that are suitable for the SPR based sensing technique [2]. Jain et al. investigated the absorption and scattering properties of gold nanoparticles of different sizes, using the Mie theory with its importance in biological imaging and biomedicine applications [3]. Dhawan et al. analyzed the characteristics of plasmonics-active metals of nanosphere dimers for the electromagnetic fields and compared them using the Finite Difference Time Domain (FDTD). In this study, electromagnetic fields and retardation effects were solved completely using Maxwell's equations and FDTD [4]. Norton et al. developed algorithms to calculate the electric field surrounding the metal nanospheres and nanospheroids, and simulated the large electric field due to the SPR in the gap between silver nanoparticles [5]. Many researchers developed various models for studying the interactions between electromagnetic waves and nanostructures like nanoshells and nanospheroids using the FDTD and FEM analysis. [4-7]. Puckett et al. observed the color change of gold nanoparticles, while interacting with ozone in a cyclic manner that was evident from the UV-Visible frequency shift [8]. Pisarenko et al. developed gold nanoislands, and observed the SPR shift at a very low ozone concentration of 20 µg/L [9]. Belaqziz et al. fabricated an SnO_2 thin film sensor using a sol-gel process, that exhibited 3.5 times enhanced response of ozone detection for 500 ppb of ozone concentration at room temperature [10]. Rahmat et al. fabricated a multi-layer photonic crystal for the detection of ozone using the sol-gel method, and the performance of the crystal was analyzed spectroscopically [11]. An ozone sensor using tungsten oxide thin films was developed with and without interrupting the sputtering process, by Vallejos et al., and it was found that the interrupted thin films exhibited enhanced the response towards ozone sensing over the others [12]. Ebeling et al. developed and characterized an ozone sensor and related instrumentation for analyzing and optimizing various parameters related with electrochemical ozone sensing [13]. Chien et al. investigated the detection of ozone concentration of 1 ppm to 2.5 ppm range, using ZnO nanorods in terms of response and recovery time of the nanosensor [14]. Wang et al. demonstrated the characteristics of a photo-simulated ozone sensor, based on indium oxide nanoparticles for ozone monitoring in air and water treatment applications [15, 16]. Acuautla et al. fabricated ZnO based flexible ozone sensors employing photolithography, and the laser ablation method that exhibited good stability, fast response/recovery and excellent detection limit from 5 ppb to 300 ppb [17].

Previously, we developed a simple optical sensor for the detection of ozone using gold and silver thin film

nanoislands that exhibited an optimum detection limit [18]. In this work, we have developed an Au@Ag core-shell thin film nanoislands ozone sensor, using APTMS and PVA binding methods in order to enhance the sensing. The simulation and analysis of the proposed sensor using COMSOL Multiphysics 4.2 and MATLAB, is presented in Section 2. Section 3 describes the fabrication details of the proposed sensors, employing APTMS and PVA binding methods. The fabricated sensor responses based on the absorption of ozone, analyzed through UV-Visible spectroscopy, SEM and AFM, and the details are given in Section 4. Further, the performance of the fabricated Au@Ag core-shell sensor responses was compared with that of the simple Au/Ag ozone sensor, developed in our previous work and reported in [18].

2. Simulation and analysis of Au@Ag core-shell thin film nanoislands

In our previous work [18], the change in the Surface Plasmon Resonance (SPR) shift on gold and silver thin film nanoislands due to ozone absorbance was simulated and analyzed, using the Mie theory. In this paper, we have extended the work to enhance the ozone detection ability of thin film nanoislands, by depositing Au@Ag core-shell nanoislands instead of a simple Au or Ag based sensor. The core-shell configuration showed enhanced performance in ozone detection. Figure 1(A) shows the schematic representation of the Au@Ag core-shell nanoislands. When UV-light falls on the Au@Ag core-shell thin film nanoislands, it propagates along the thin film deposited on the glass substrate. The analytical equation employed to estimate the extinction coefficient is given by

$$Q_{ext} = \frac{8\pi^2 R_s^3}{\lambda\sqrt{\varepsilon_{ozone}}}\mathrm{Im}\left(\varepsilon_{ozone}\frac{(R_s/R_c)^3(2\varepsilon_s+\varepsilon_c)(\varepsilon_s-\varepsilon_{ozone})-(\varepsilon_s-\varepsilon_c)(2\varepsilon_s+\varepsilon_{ozone})}{(R_s/R_c)^3(2\varepsilon_s+\varepsilon_c)(\varepsilon_s+2\varepsilon_{ozone})-(\varepsilon_s-\varepsilon_c)(\varepsilon_s-\varepsilon_{ozone})}\right)$$

where ε_c, ε_s, ε_{ozone} are the dielectric constants of the core (Au), shell (Ag) and ozone respectively. R_s/R_c is the ratio of shell radius to core radius, and *Im* stands for the imaginary part of the expression [19]. This equation was used to estimate the absorbance of light by the Au@Ag core-shell nanoparticle thin film nanoislands using MATLAB. The structure created in the COMSOL Multiphysics 4.2 environment, as per the dimensions and conditions employed for our previous model was based on gold and silver thin film nanoislands in [18]. Both the simulation and analysis were performed in DELL Inspiron 4010 Laptop with Core i3, 2.13 GHz processor, 4 GB RAM and Windows 7 home basic operating system. The dimensions of the model were taken as 1 cm x 1 cm x 0.1 cm and 1 cm x 1 cm x 0.1 µm for the glass plate and the thin film nanoislands, respectively. Figure 1(B) gives a clearer view of the dimensional analysis of the model. The x, y and z-axes represent the length, breadth and height of the glass. The top layer is either the APTMS Au@Ag core-shell thin film nanoislands or the PVA thin film nanoislands.

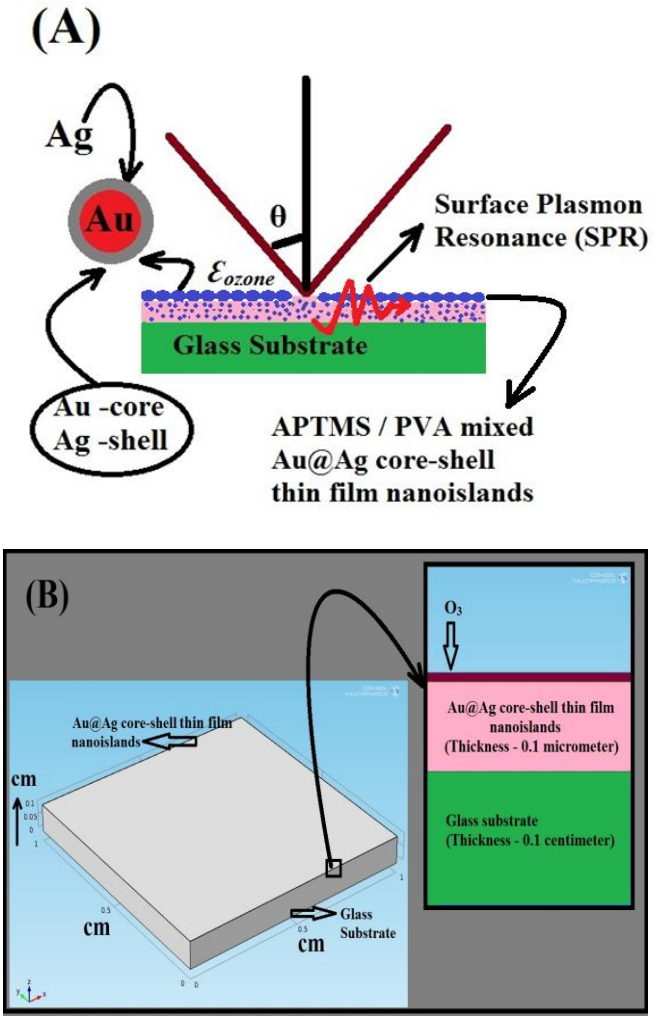

Figure 1: (A) Schematic proposed model diagram with SPR shift along thin film (B) Proposed model dimensions of Au@Ag core-shell nanoislands on the glass plate.

The 3D model was implemented using the physics equations, meshing and plotting of the model in the graphics window. The boundary conditions are implemented in the proposed model in terms of Partial Differential Equations. The model was analyzed using the meshing technique; i.e. the model was divided into small sections for better estimation of results, by way of applying the boundary conditions to each element of the structure [18]. A finer mesh leads to high-quality results for the model. The number of elements varies, based on the different meshed element size like, coarse, fine and extremely fine. The element sizes for the extremely fine, finer, and coarse meshes are 663598, 340586, and 273398, respectively. The extremely fine mesh model

requires more time and memory for the computation of the results but gives high- quality results for the various boundary conditions. In this study, we implemented fine meshing in the proposed model for the estimation of the various analyses as shown in Figure 2.

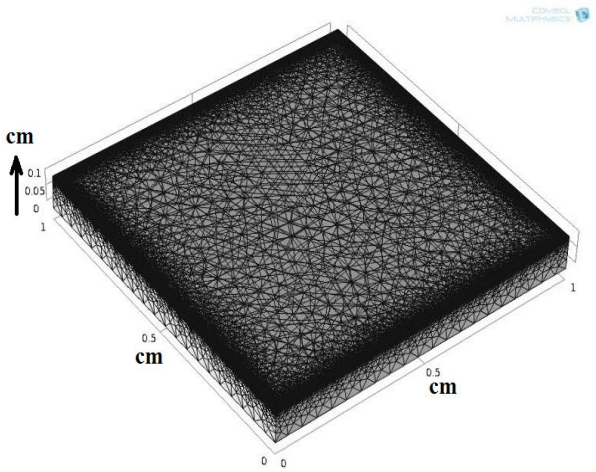

Figure 2: A view of the extremely fine meshed image of Au@Ag core-shell thin film nanoislands.

When UV-light falls on the Au@Ag core-shell thin film nanoislands, the light passes along the thin film nanoislands due to the Surface Plasmon Resonance (SPR). An appreciable color change is observed, due to the interaction of the UV-light on the APTMS and PVA based Au@Ag core-shell thin film nanoislands, as shown in Figures 3(A) and 3(B), respectively. Further, it was observed that the color variations in the APTMS Au@Ag core-shell thin film nanoislands was found to be distinct in each section, as shown in Figure 3(A). On the other hand uniform color variations were observed in PVA mixed Au@Ag core-shell thin film nanoislands as shown in Figure 3(B), which may represent the non-linear absorbance of ozone by the sensor binding materials.

Figure 4(A) shows the UV absorbance spectra of APTMS Au@Ag core-shell thin film nanoislands before ozonation; the absorbance peaks appear at 375 nm and 480 nm corresponding to the SPR shifts of Ag and Au nanoparticles respectively. Further, the SPR shifts of the Ag and Au nanoislands increase from 0.21 to 0.27 and 0.25 to 0.33 respectively, when exposed to ozone, which clearly showed a measurable change in the absorbance responses of the sensor materials. Similarly, in the PVA mixed Au@Ag core-shell thin film nanoislands, the shifts occur at 380 nm and 490 nm. When exposed to UV light, there was an increase in SPR shifts from 0.36 to 0.42 and from 0.35 to 0.41 noticed for the Ag and Au nanoislands after ozonation, as is evident from Figure 4(B). It is further observed from Figure 4(B) that there was a slight reduction in the absorbance peaks for PVA mixed Au@Ag core-shell thin film nanoislands due to the polymer matrix attenuation. The simulation results revealed that the Au@Ag core-shell thin film nanoislands were found to be very sensitive towards ozone detection, and were suitable material for the fabrication of nanosensors. Further, the polymer binding methods, such as APTMS and PVA improved the bonding between the substrate and the sensing materials as well as the uniform coating of the nanolayers.

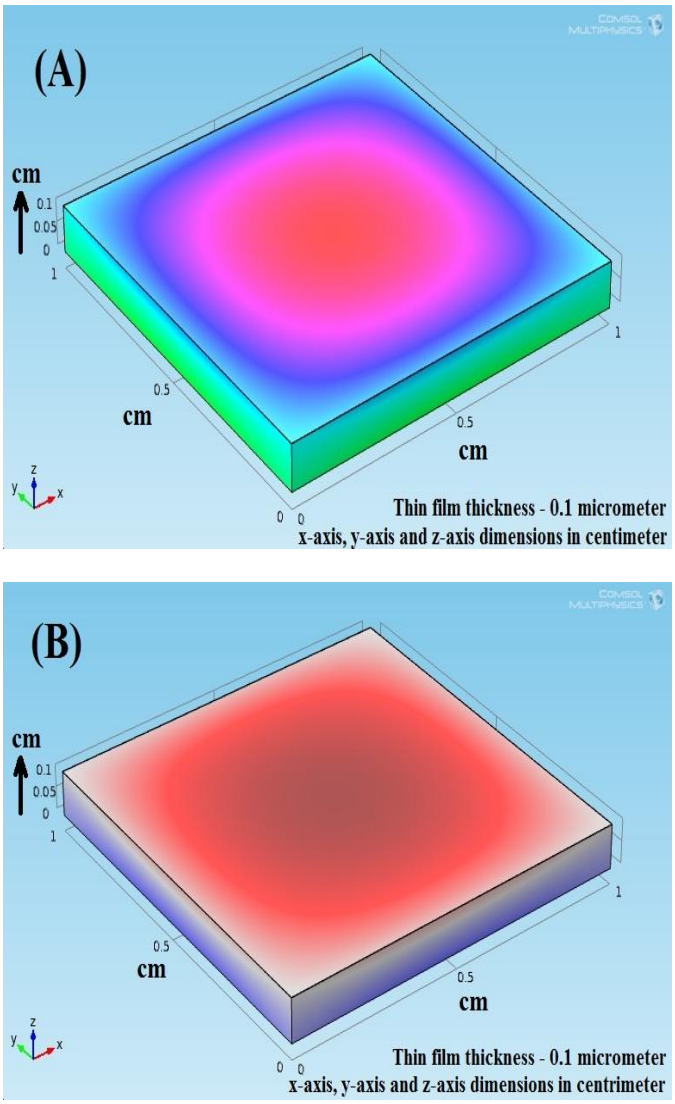

Figure.3: Simulated SPR Images of (A) APTMS Au@Ag core-shell thin film nanoislands and (B) PVA Mixed Au@Ag core-shell thin film nanoislands.

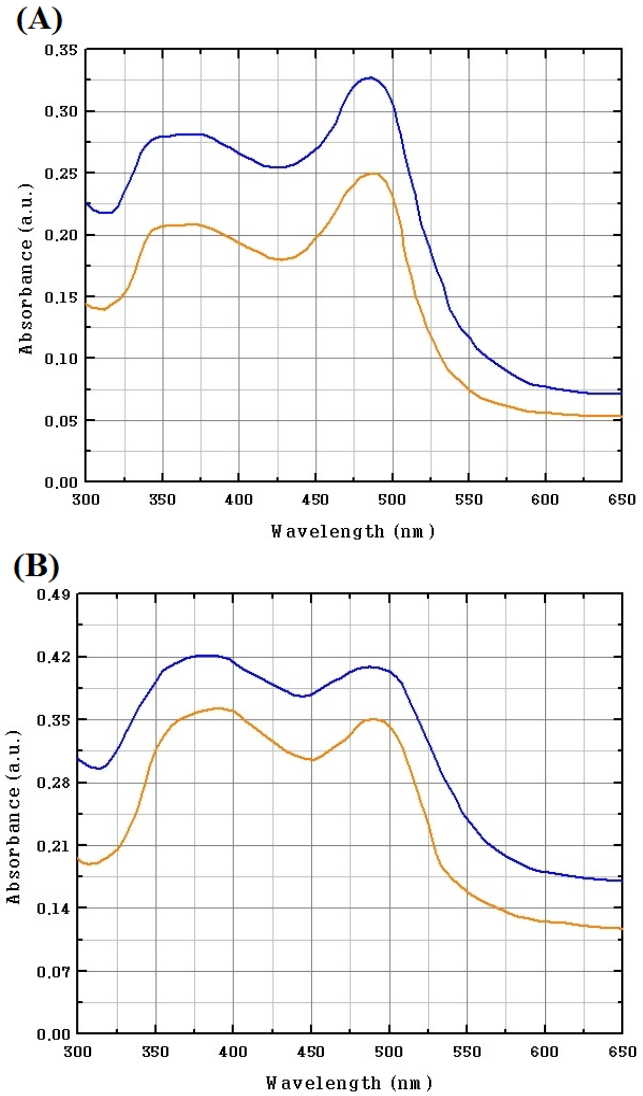

Figure 4: Simulation graphs of ozone absorbance on the (A) APTMS core-shell thin film nanoislands and (B) PVA mixed Au@Ag core-shell thin film nanoislands.

3 Synthesis of Au@Ag core-shell thin film nanoislands

Based on the simulation results presented in Section 2, the fabrication of Au@Ag core-shell thin film nanoislands using APTMS and PVA binding methods, was carried out in this work.

3.1 Materials

The chemicals $HAuCl_4$ and chromic acid were purchased from Sigma-Aldrich. APTMS was procured from Lancaster, UK. All other chemicals were brought from local commercial sources. Ultrapure water with the resistivity of 18 MΩ (Milli-Q-Water, Millipore System) was used for all the synthesis work involved in this study.

3.2 APTMS Method

In this method, the Au@Ag core-shell thin film nanoislands were fabricated on a BK7 glass substrate by following the chemical route given in the sub-sections below.

3.2.1 Synthesis of Gold Nanoparticles

In 150 mL Milli-Q water, 2.2 mM trisodium citrate was added and boiled with continuous stirring. In this boiling mixture, 1mL of 25 mM $HAuCl_4$ was injected after 15 min. Then, the solution was cooled for 10 min in order to reach a temperature of 90 $^{\circ}$C. Again, 1mL of a 25 mM of $HAuCl_4$ aqueous solution was added to the mixture. After 30 min, 55 mL of the mixture was extracted. Then, 2.2 mL of 60 mM sodium citrate and 53 mL of water werea added. This solution was used as the seed solution. The above procedure was repeated three to five times to obtain 32 and 55 nm Au nanoparticles [20].

3.2.2 Synthesis of Au@Ag core-shell Nanoparticles

10 mL of Au nanoparticle solution, 75 µL of NaOH (100 mM), 15 µL of $AgNO_3$ (100 mM) and 60 µL of Ascorbic Acid (100 mM) were added in a beaker and boiled. The boiling solution was stirred for 30 min continuously, and again solutions of 15 µL of $AgNO_3$ (100 mM), 75 µL of NaOH (100 mM) and 60 µL of Ascorbic Acid (100 mM) were added. The mixture was centrifuged and redispersed in water [20].

3.2.3 Synthesis of Silver Nanoparticles

The citrate reduction method was used for synthesizing the Ag nanoparticles. Deionized water (100 mL) was added to 4.5 mg of $AgNO_3$ and boiled. To this boiling solution, 12 mL of 1% sodium citrate solution was added. The boiling was maintained for 1 h in order to obtain ~70 nm diameter Ag nanoparticles, [20].

3.2.4 Glass Substrate Cleaning

Initially, the glass plates were cleaned with a chromic acid solution ($K_2Cr_2O_7$:H_2SO_4) for removing the dust particles and metal ions. Then, the substrates were cleaned with deionized water. Then, Piranha cleaning, prepared by mixing 70% of H_2O_2 in 30% of H_2SO_4, was used to remove the organic impurities, and rinsed with DI water [21]. Nitrogen gas was used for removing the wetness on the samples.

3.2.5 APTMS binding modification on glass substrates

A solution of 0.3 mL of APTMS in 3ml of ethanol was prepared. The prepared solution was taken in a Petridish. The glass slides were kept in the prepared solution for 12 hour and dried with nitrogen. As the APTMS forms an adhesive layer on the top of the glass substrate, it provides good binding for the nanoparticles with the surface [21]. For depositing the Au@Ag core-shell nanoislands on the surface of the modified glass plates, they were kept in the Au@Ag core-shell nanoparticle solution for about 12 to 18 hours to obtain a uniform layer throughout the substrates. Thus, the APTMS binding Au@Ag core-shell thin film nanoislands were deposited on the BK7 glass plates.

3.3 PVA Method

In this method, the Au@Ag core-shell thin film nanoislands were fabricated on the BK7 glass plate. The fabrication of the PVA mixed Au@Ag core-shell thin film nanoislands is described in the following sub-sections.

3.3.1 Preparation of PVA mixed Au@Ag core-shell solution

The preparation of the PVA mixed silver nanoparticle solution [22] is similar procedure to the one implemented for fabricating Au@Ag core-shell thin film nanoislands. In this method, the PVA was mixed with ethanol and a pinch of NaCl to form a colloidal solution. NaCl acts as a conducting layer to measure the resistivity measurements. Then, the PVA colloidal solution was mixed with the Au@Ag core-shell nanoparticles. The solution was stirred continuously for the duration of 15 min to form a uniform distribution of Au@Ag core-shell nanoparticles. Thus, the PVA mixed Au@Ag core-shell colloidal solution was formed by depositing the thin film nanoislands on the glass substrate.

3.3.2 Deposition of the PVA mixed Au@Ag core-shell thin film nanoislands

Here, the PVA mixed Au@Ag Core-shell thin film nanoislands was deposited on the BK7 glass substrate using a spin coating technique [22]. The experiment was carried out in a dark room to protect the samples from the photoluminescence effect. The deposited thin film nanoislands were dried by keeping them on a hot plate maintained at 100 oC. Finally, the PVA mixed Au@Ag thin film nanoislands were prepared for ozone sensing and characterization.

3.4 Glass substrates storage after deposition

To avoid contamination from dust and environmental gases; the samples were stored in a Petridish. Even though, the Au@Ag core-shell is a noble metal, it reacts with light (Photoluminescence effect). Therefore, the Petridish was covered with a Mylar sheet and tightly closed to avoid contamination of the samples by other natural gases.

4. Instrumentation

For testing the ozone sensing of the fabricated APTMS/PVA binding based Au@Ag core-shell thin film nanoislands, a corona discharge ozone generator was employed. The ozone generator comprises of an ozone cell, high voltage generator (6 kV to 7 kV) and air preparation unit. In the air preparation unit, the air was initially compressed by a small air compressor and fed through a dryer for removing the moisture present in the air. Then, the air was fed into the ozone cell made up of an inner metal electrode and outer glass electrode with an air gap of 0.8 mm between these two electrodes. The air fed into the gap was subjected to a high-voltage corona discharge, that split the O2 molecule into two O atoms, which in turn, combined with another O2 molecule and resulted in the O3 molecule. The capacity of the ozone generator used for testing the sensor materials is 1 g/h.

For analyzing the UV absorbance responses of the Au@Ag core-shell thin film nanoislands before and after ozone contacting, a 1 nm resolution UV-Visible spectrophotometer was used for analyzing optical responses. The Au@Ag core-shell thin film nanoislands coated glass plates were kept in the sample holder to analyze the absorbance. The background spectrum was corrected by placing the uncoated glass plates in the sample holder before taking the coated sample measurements.

SEM and AFM microscopes were used for analyzing the surface morphology of the fabricated Au@Ag core-shell thin film nanoislands samples. In AFM (Park XE-100), the non-contact mode was used for analyzing the roughness morphology of the thin film nanoislands, using Si3N4 cantilevers. SEM (Hitachi S-4700) was used for analyzing the samples.

5. Testing Details

The chamber used for testing the fabricated sensor materials is shown in Figure 5; it has an inlet and an outlet with regulating valves for controlling the flow rate of ozone. Initially, the chamber was connected to a vacuum pump for removing the residual air from the chamber. Then, the sensor was fixed at the center of the chamber for

ozone contacting. There is a provision in the chamber for connecting a multimeter with the sensor material for resistivity measurements. For resistivity measurements, the Agilent Model 34401A digital multimeter was employed. The probes of the multimeter were connected to the edges of the thin film to analyze the ozone response in terms of resistivity. The resistivity, before and after passing ozone gas, was analyzed for verifying the variations in resistivity, with respect to the ozone gas absorption on the Au@Ag core-shell thin film nanoislands. After removing the residual air from the chamber and fixing the sensor for testing, ozone gas was allowed through the chamber. For estimating the ozone gas concentration in the testing chamber, the outlet of the testing chamber was connected to an ozone analyzer (BMT Model 964), which displayed the ozone concentration in the chamber. An electric heater was kept below the glass substrate to analyze the resistivity variations on the thin film nanoislands with respect to temperature. A profilometer was used to verify the thickness of the APTMS/PVA binding based Au@Ag core-shell thin film, which was found to be ~0.1 µm.

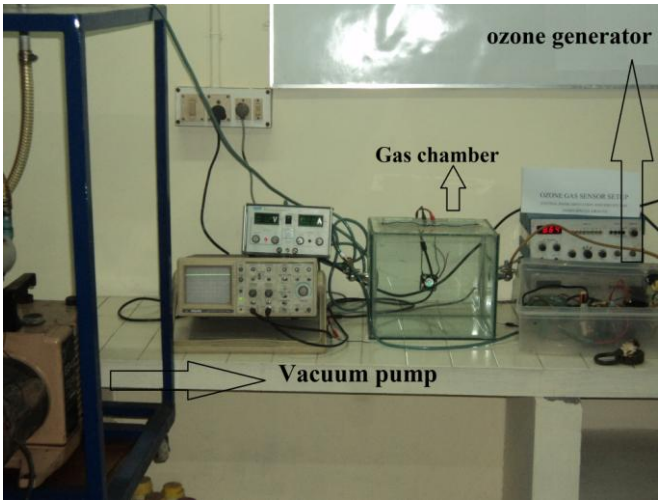

Figure 5: Experimental set-up for testing Au@Ag core-shell thin film nanoislands.

6. Sensor Characterization

For characterizing both the APTMS and PVA binding Au@Ag core-shell thin film nanoislands, the optical and resistive responses of the fabricated sensors were studied. The optical and resistive responses measured using the UV-Visible spectroscopy and digital multimeter respectively are summarized as follows.

6.1 Optical Responses

Figure 6 shows the absorbance peaks of APTMS Au@Ag core-shell thin film nanoislands, with different dosages of ozone and without ozonation.

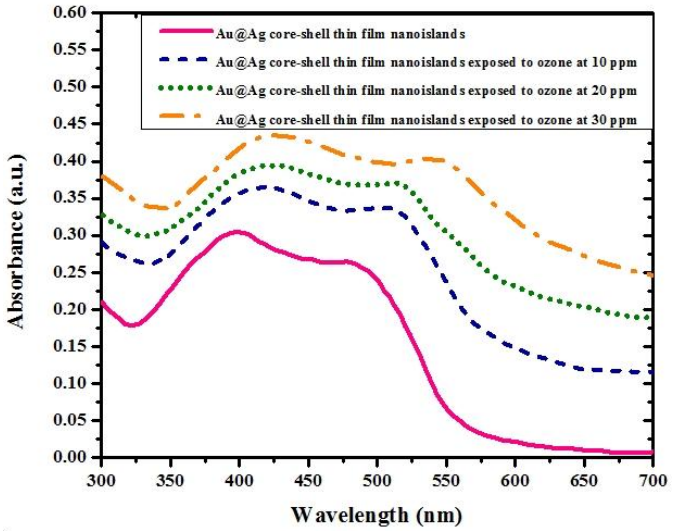

Figure 6: UV-Visible spectra of Au@Ag core-shell thin film nanoislands before (continuous line) and after ozonation (dotted lines)

The SPR peaks for Ag and Au without ozonation, were found at 380 nm and 490 nm respectively. After ozonation, there was an increase in the absorbance peak amplitudes from 0.30 to 0.35 at 400 nm and 0.25 to 0.32 at 510 nm, noticed for the APTMS Au@Ag core-shell thin film nanoislands. The detection of ozone due to the absorbance was found at 10 ppm. Further, the absorbance peaks for the Ag and Au were found to increase with ozone concentration from 10 ppm to 20 ppm to 30 ppm. In simulation, the absorbance peaks were found to be very sharp and occurred at 375 nm and 480 nm for the Ag and Au, respectively. On the other hand, the fabricated sensor's absorbance peaks were found to be similar, and occurred at 380 nm and 490 nm, for the Ag and Au, respectively. It may be due to the effect of the APTMS binding material's absorbance of the UV radiation. Further, the sensor materials exposed to other gases like O_2, H_2 and N_2, and there was no measurable change in the absorbance peaks; that is, the sensors were selective to ozone gas only.

Without ozonation, the absorbance peaks appeared at 390 nm and 530 nm for the Ag and Au, whereas there was a shift in absorbance peaks from 0.08 to 0.10 at 410 nm and 0.10 to 0.13 at 530 nm found for Ag and Au, when the sensor materials were exposed to the ozone dosage of 35 ppm. Further, the peaks were found to increase while increasing the ozone dosage from 35 ppm to 40 ppm to 45 ppm, which indicated that the sensor materials were sensitive to the increase in ozone dosage. The sensor materials were tested for other gases like O_2, N_2, and H_2, and there was no measurable change in the absorbance peaks, which means that the sensors were selective only to ozone gas.

Figure 7 shows the UV absorbance spectra of PVA mixed Au@Ag core-shell thin film nanoislands before and after ozonation.

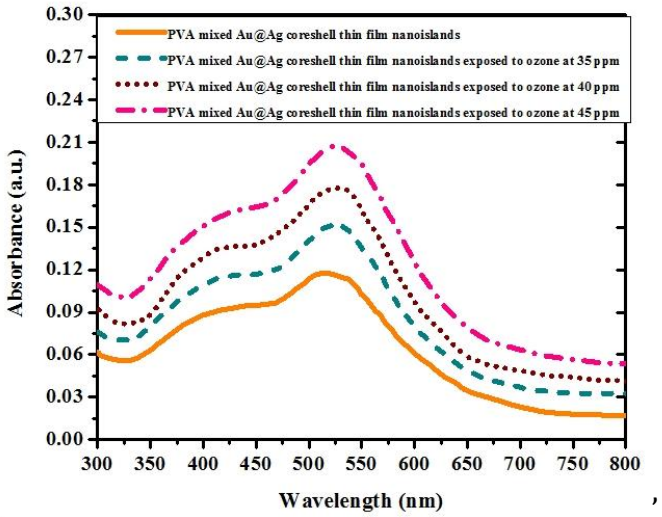

Figure 7: UV-Visible absorption spectra of PVA mixed Au@Ag core-shell thin film nanoislands before (continuous line) and after ozonation (dotted lines).

From Figures 6 and 7, it is seen that PVA mixed Au@Ag core-shell nanoislands have sharper peaks for Au than APTMS Au@Ag core-shell nanoislands. It is found that PVA mixed nanoislands exhibited a measurable peak value for the ozone dosage of 35 ppm, than the APTMS nanoislands which were found to respond very well even for the lower ozone dosage level of 10 ppm. As a result, the fabricated APTMS Au@Ag core-shell thin film nanoislands detected the ozone better than the PVA mixed Au@Ag core-shell thin film nanoislands. Moreover, Au responded better than Ag in both the APTMS and PVA bindings, which is evident from the ozone absorbance responses shown in Figures 6 and 7. Further, the absorbance responses of the Au@Ag core-shell thin film nanoislands were more effective for ozone detection than the simple Au/Ag nanoislands, which is evident from the results obtained in our previous study [18].

6.2 Resistive Responses

The resistance responses of the APTMS/PVA based Au@Ag core-shell thin film nanoislands before and after ozonation, were studied and are shown in Figure 8. In both the materials, the resistivity was found to increase with ozone concentration due to the absorbance of ozone on Au@Ag core-shell thin film nanoislands. But, the APTMS Au@Ag core-shell nanoislands were found to be more resistive than the PVA mixed Au@Ag core-shell nanoislands. This may be due to the efficient ozone absorbance and low polymer matrix attenuation of the APTMS than the PVA. In this study, the resistive responses of the Au@Ag core-shell thin film nanoislands were found to be more sensitive than those of the simple Au/Ag thin films results reported in [18]. Figure 9 shows the resistance responses of the fabricated sensors with respect to temperature variations. It is also evident that APTMS Au@Ag core-shell thin film nanoislands exhibited more linear responses than the PVA nanoislands, because of the high electron flow of the APTMS nanoislands.

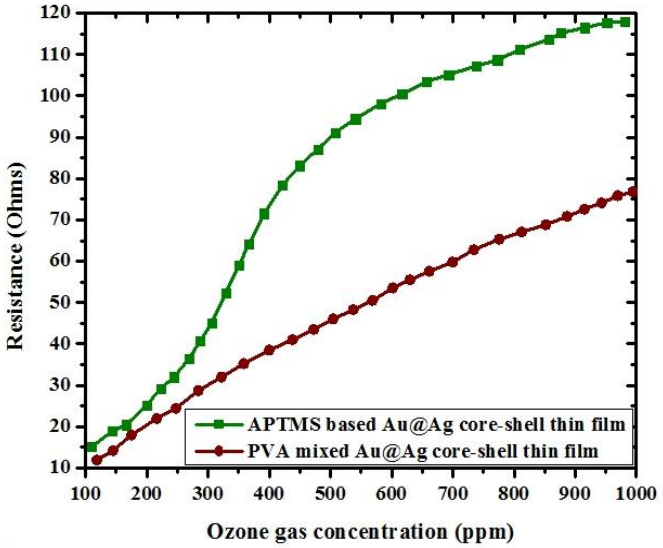

Figure 8: Resistance (Ohms) response for different ozone concentrations (ppm) of Au@Ag core-shell thin film nanoislands

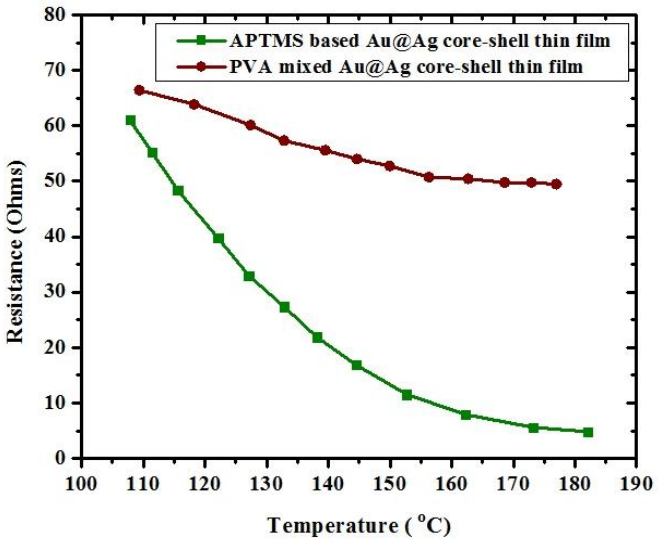

Figure 9: Resistance (Ohms) response with respect to temperature (ºC) variations of Au@Ag core-shell thin film nanoislands.

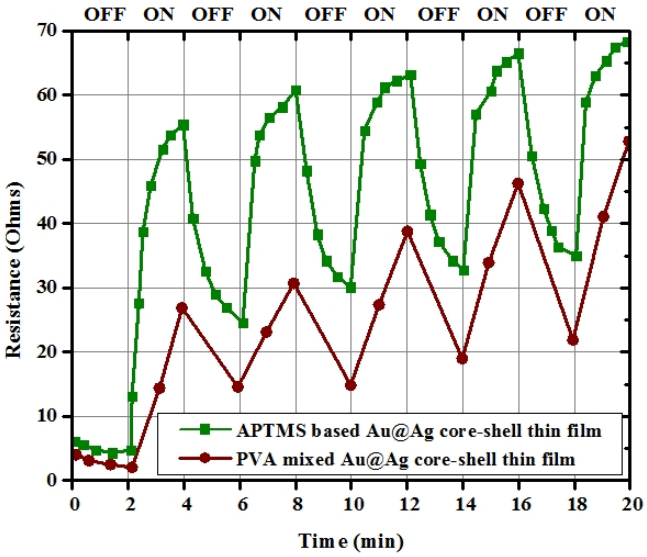

Figure 10: Repeatability and reversibility responses of Au@Ag core-shell thin film nanoislands.

To study the repeatability and reversibility responses of the APTMS/PVA based Au@Ag core-shell thin film nanoislands, ON and OFF states were created by passing and removing the ozone gas in a cyclic manner [18]. From Figure 10, a reversible response and incomplete recovery were noticed for both the APTMS and PVA binding Au@Ag core-shell thin film nanoislands. Further, it was found that the APTMS Au@Ag core-shell thin film nanoislands were found to be highly responsive to ozone dosage, than the PVA mixed Au@Ag core-shell thin film nanoislands.

From the above studies, both the optical and resistive responses of the APTMS and PVA based Au@Ag core-shell thin film nanoislands are found to be good for ozone detection. Compared with our previous results [18], APTMS/PVA based Au@Ag core-shell thin film nanoislands are found to have better responses for the detection of ozone than Au/Ag thin film nanoislands.

7. SEM Analysis

Figure 11 shows the SEM images of the APTMS Au@Ag core-shell thin film nanoislands before and after ozonation. Before ozonation, highly crystalline spherical nanoislands were observed, whereas the spherical structure was found to be distorted after ozonation due to the absorbance of ozone on the Au@Ag core-shell thin film nanoislands. For the PVA mixed Au@Ag core-shell thin film nanoislands, the Au@Ag core-shell nanoislands were embedded into the PVA polymer matrix as shown in Figure 12. But this embedded structure faded fully due to the absorbance of ozone on thin film nanoislands. In both the cases, the Au@Ag core-shell thin film nanoislands absorbed the ozone gas uniformly; this was evident from the SEM images shown in Figures 11 and 12.

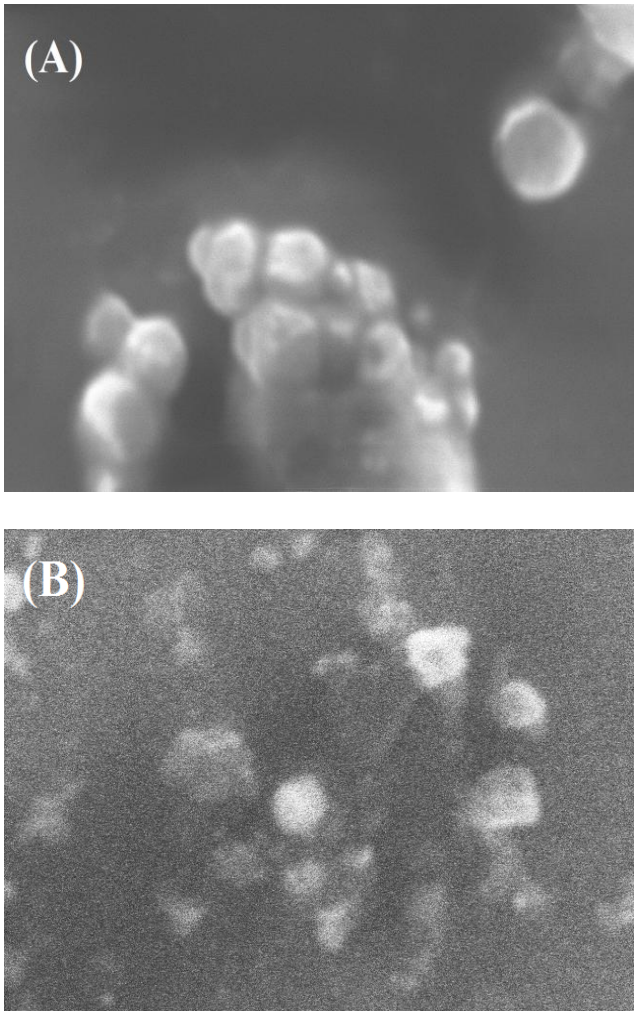

Figure 11: SEM images of APTMS Au@Ag core-shell thin film nanoislands (A) before and (B) after ozonation.

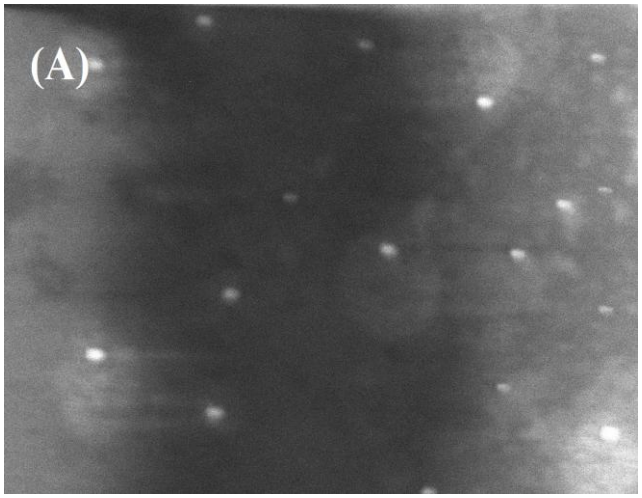

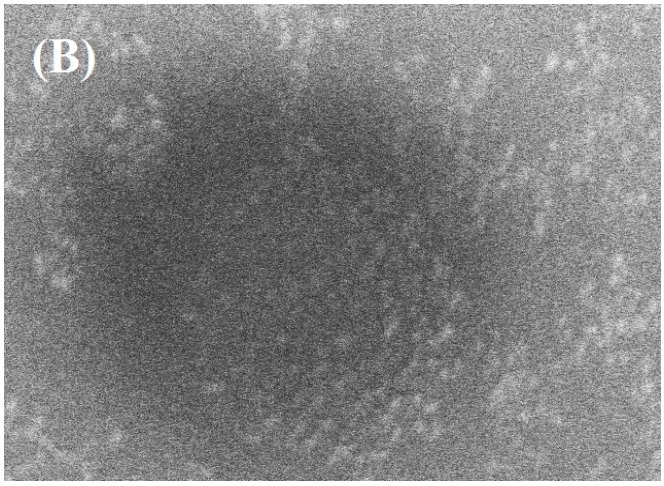

Figure 12: SEM images of PVA mixed Au@Ag core-shell thin film nanoislands (A) before and (B) after ozonation.

8. AFM Analysis

The AFM images of the APTMS Au@Ag core-shell thin film nanoislands are given in Figure 13. In Figure 13(A), the rough morphology of the nanoislands with grove like structures was observed before ozonation. After ozonation, the rough morphology became smooth, and uniformity was observed due to ozone absorbance on the Au@Ag nanoislands. The AFM images revealed that there was a significant variation in the morphology of the nanoislands, before and after ozonation.

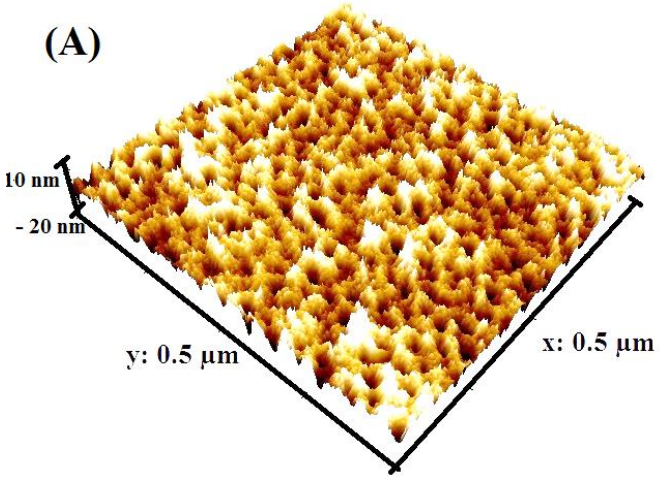

The AFM images of PVA mixed Au@Ag core-shell thin film nanoislands are shown in Figure 14. A comparison of the AFM images of both APTMS and PVA mixed nanoislands before ozonation, reveals that the PVA mixed nanoislands exhibited more roughness than the APTMS Au@Ag core-shell thin film nanoislands. Further, the PVA mixed nanoislands were found to be less smooth than the APTMS Au@Ag core-shell thin film nanoislands, due to the PVA polymer matrix. Moreover, both the APTMS/PVA based Au@Ag core-shell thin film nanoislands exhibited more distinct roughness than the APTMS/PVA Au/Ag thin film nanoislands without core-shell formation that was inferred from our previous study [18].

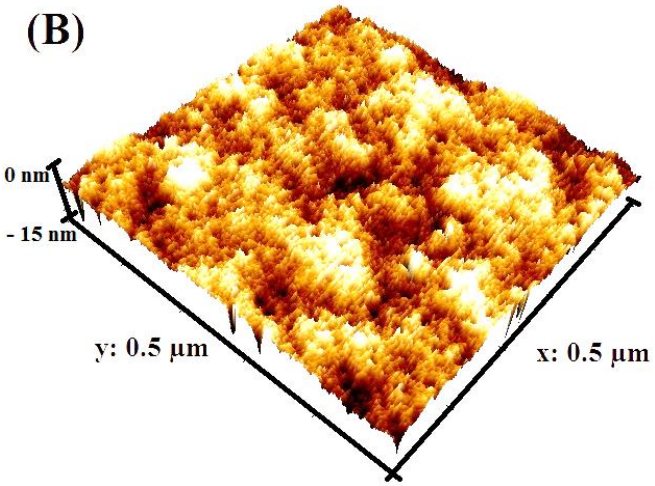

Figure 13: AFM images of APTMS Au@Ag core-shell thin film nanoislands (A) before and (B) after ozonation.

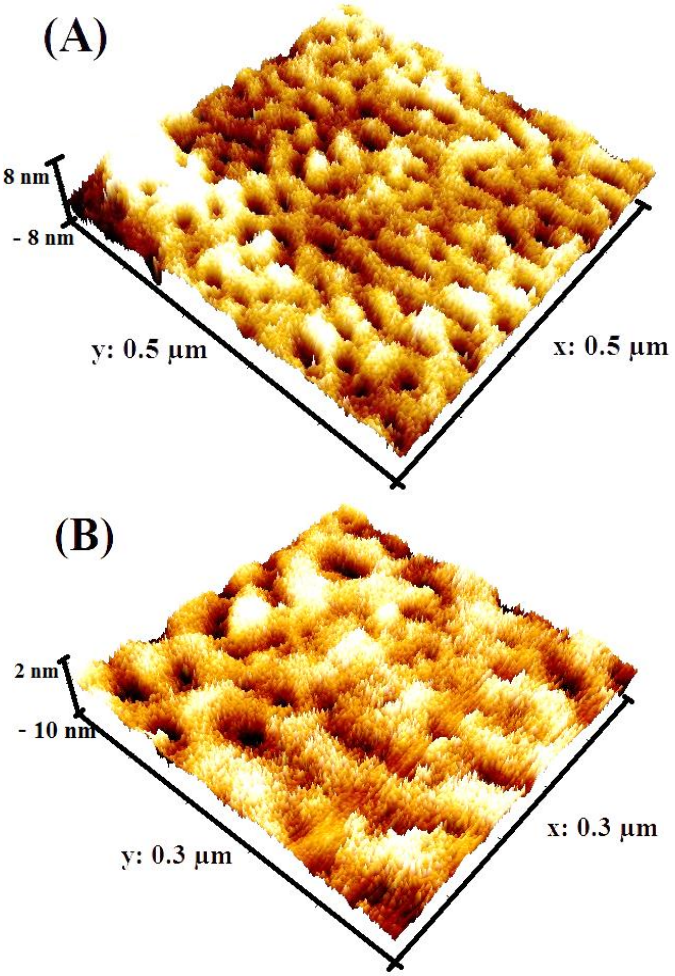

Figure 14: AFM images of PVA mixed Au@Ag core-shell thin film nanoislands (A) before and (B) after ozonation.

9. Conclusion

In this work, optical sensors using the Au@Ag core-shell thin film nanoislands with APTMS and PVA as binding agents were developed. Both the sensor structures were simulated as models in COMSOL Multiphysics 4.2, and analyzed in MATLAB software environment. Based on the simulation results, both the APTMS and PVA based models were fabricated by the chemical route. The fabricated sensor materials were characterized, using the optical, resistivity and morphological analyses. These measurements exhibited encouraging results, and it was found that the APTMS/PVA based Au@Ag core-shell thin film nanoislands performed better in ozone sensing, than the APTMS/PVA based Au/Ag thin film nanoislands, reported in [18]. From simulation and fabrication results, the APTMS Au@Ag core-shell thin film nanoislands showed better ozone sensing than the PVA mixed Au@Ag core-shell nanoislands. As a result, the APTMS Au@Ag core-shell thin film nanoislands were used as effective sensor material confirming standardization measurements like sensitivity, accuracy, resolution, repeatability, reproducibility.

Acknowledgement

This work was financially supported by the National Centre for Nanoscience and Nanotechnology (MHRD-Special Grants), the University of Madras (Grant No: C-2/Res.Pro/NSNT/Proj.No.26/ 2011/184, dated 13th May 2011). We specially thank Mr D. Manikandan, Department of Chemical Engineering, Anna University, Chennai helped a lot in the synthesis of core-shell nanoparticles. We express our special and sincere thanks to Professor Dr. R. Jayavel, Director, Centre for Nanoscience and Technology, Anna University, for extending the AFM and SEM facility for sample characterization. One of the authors (SA) expresses his sincere thanks to the Indian Nano User Program (INUP), the Indian Institute of Science (IISc-Bangalore), and the National Nano Fabrication Centre (NNFC-Cleanroom), for the support and training provided to fabricate MEMS devices. We thank the National MEMS Design Centre (NPMASS Funding), Rajalakshmi Engineering College, for its support in providing the software facility. We thank Prof. P. R. Subramanian, Emeritus Professor, Dept of CISL, University of Madras, for carrying out the language correction of this manuscript.

REFERENCES

[1] Wolfbeis O. S, and Homola J, Surface Plasmon Resonance Based Sensors, Springer, 2006, http://dx.doi.org/10.1007/b100321

[2] Louis C and Pluchery O, Gold Nanoparticles, Physics, Chemistry and Biology, Imperial College Press, London, 2012, ISBN 978-1-84816-806-0, http://dx.doi.org/10.1002/anie.201309807

[3] Jain P.K, Lee K.S, El-Sayed I.H, El-Sayed M.A, Calculated absorption and scattering properties of gold nanoparticles of different size, shape, and com-position: applications in biological imaging and biomedicine, J. Phys. Chem. B110 (2006) 7238–7248, http://dx.doi.org/10.1021/jp057170o

[4] Dhawan, A., Norton, S. J., Gerhold, M. D., & Vo-Dinh, T. Comparison of FDTD numerical computations and analytical multipole expansion method forplasmonics-active nanosphere dimers. Optics Express, 17(12), (2009) 9688-9703. http://dx.doi.org/10.1364/oe.17.009688

[5] Norton, S. J., & Vo-Dinh, T. Optical response of linear chains of metal nanospheres and nanospheroids. Journal of the Optical Society of America A, 25(11), (2008) 2767-2775. http://dx.doi.org/10.1364/josaa.25.002767

[6] Chau, Y.-F., Yeh, H.-H., & Tsai, D. P. Surface plasmon effects excitation from three-pair arrays of silver-shell nanocylinders. Physics of Plasmas, 16(2), (2009) 022303. http://dx.doi.org/10.1063/1.3068469

[7] Khoury, C. G., Norton, S. J., & Vo-Dinh, T. Plasmonics of 3-D Nanoshell Dimers Using Multipole Expansion and Finite Element Method. ACS Nano, 3(9),(2009) 2776-2788. http://dx.doi.org/10.1021/nn900664j

[8] Puckett S.D, Heuser J.A, Keith J.D, Spendel W.U, Pacey. G.E, Interaction of Ozone with Gold Nanoparticles, Talanta 66 (2005) 1242–1246. http://dx.doi.org/10.1016/j.talanta.2005.01.038

[9] Aleksey N. Pisarenko, Wolfgang U. Spendel, Richard T. Taylor, Jordan D. Brown, James. A. Cox, Gilbert E. Pacey, Detection of ozone gas using gold nanoislands and surface plasmon resonance, Talanta 80 (2009) 777–780. http://dx.doi.org/10.1016/j.talanta.2009.07.062

[10] Belaqziz, M., Amjoud, M. b., Gaddari, A., Rhouta, B., & Mezzane, D. Enhanced room temperature ozone response of SnO2 thin film sensor. Superlattices and Microstructures, 71(0), (2014)185-189. http://dx.doi.org/10.1016/j.spmi.2014.03.040

[11] Rahmat, M., Maulina, W., Isnaeni, Miftah, D. Y. N., Sukmawati, N., Rustami, E., Alatas, H. Development of a novel ozone gas sensor based on sol–gel fabricated photonic crystal. Sensors and Actuators A: Physical, 220(0), (2014) 53-61. http://dx.doi.org/10.1016/j.sna.2014.09.020

[12] Vallejos, S., Khatko, V., Aguir, K., Ngo, K. A., Calderer, J., Gràcia, I., Correig, X. Ozone monitoring by micro-machined sensors with WO3 sensing films. Sensors and Actuators B: Chemical, 126(2), (2007) 573-578. http://dx.doi.org/10.1016/j.snb.2007.04.012

[13] Ebeling, D., Patel, V., Findlay, M., & Stetter, J. (2009). Electrochemical ozone sensor and instrument with characterization of the electrode and gas flow effects. Sensors and Actuators B: Chem137(1), (2009) 129-133. http://dx.doi.org/10.1016/j.snb.2008.10.038

[14] Chien, F. S.-S., Wang, C.-R., Chan, Y.-L., Lin, H.-L., Chen, M.-H., & Wu, R.-J. Fast-response ozone sensor with ZnO nanorods grown by chemical vapor deposition. Sensors and Actuators B: Chem, 144(1), (2010) 120-125. http://dx.doi.org/10.1016/j.snb.2009.10.043

[15] Wang, C. Y., Becker, R. W., Passow, T., Pletschen, W., Köhler, K., Cimalla, V., & Ambacher, O. (2011). Photon stimulated sensor based on indium oxide nanoparticles I: Wide-concentration-range ozone monitoring in air. Sens and Actuators B: Chem, 152(2), (2011), 235-240. http://dx.doi.org/10.1016/j.snb.2010.12.014

[16] Wang, C. Y., Bagchi, S., Bitterling, M., Becker, R. W., Köhler, K., Cimalla, V., .Chaumette, C. Photon stimulated ozone sensor based on indium oxide nanoparticles II: Ozone monitoring in humidity and water environments. Sensors and Actuators B: Chemical, 164(1), (2012) 37-42. http://dx.doi.org/10.1016/j.snb.2012.01.058

[17] Acuautla, M., Bernardini, S., Gallais, L., Fiorido, T., Patout, L., & Bendahan, M. (2014). Ozone flexible sensors fabricated by photolithography and laser ablation processes based on ZnO nanoparticles. Sensors and Actuators B: Chemical, 203(0), (2014) 602-611. http://dx.doi.org/10.1016/j.snb.2014.07.010

[18] Addanki, S., Jayachandiran, J., Pandian, K., & Nedumaran, D. Development of optical sensors for the quantitative detection of ozone using gold and silver thin film nanoislands. Sensors and Actuators B: Chemical, 210(0), (2015) 17-27. http://dx.doi.org/10.1016/j.snb.2014.12.071

[19] Kuzma, A., Weis, M., Daricek, M., Uhrik, J., Horinek, F., Donoval, M., Donoval, D. Plasmonic properties of Au-Ag nanoparticles: Distinctiveness of metal arrangements by optical study. Journal of Applied Physics, 115(5), (2014) 053517. http://dx.doi.org/10.1063/1.4864428

[20] Samal, A. K., Polavarapu, L., Rodal-Cedeira, S., Liz-Marzán, L. M., Pérez-Juste, J., & Pastoriza-Santos, I. Size Tunable Au@Ag Core–Shell Nanoparticles: Synthesis and Surface-Enhanced Raman Scattering Properties. Langmuir, 29(48), (2013) 15076-15082. http://dx.doi.org/10.1021/la403707j

[21] Shakila, V., & Pandian, K. Preparation of gold nanoislands on various functionalized polymer-modified glass and ITO for electrochemical characterization of monolayer assembly of alkanethiols. Journal of Solid State Electrochemistry, 11(2), (2007) 296-302. http://dx.doi.org/10.1007/s10008-006-0107-1

[22] Gradess, R., Abargues, R., Habbou, A., Canet-Ferrer, J., Pedrueza, E., Russell, A., Martinez-Pastor, J. P. Localized surface plasmon resonance sensor based on Ag-PVA nanocomposite thin films. Journal of Materials Chemistry, 19(48), (2009) 9233-9240. http://dx.doi.org/10.1039/b910020bS.